ARTICLE

ACS chemical biology

Antagonists of the EP_3 Receptor for Prostaglandin E_2 Are Novel Antiplatelet Agents That Do Not Prolong Bleeding

Jasbir Singh[†], Wayne Zeller[†], Nian Zhou[†], Georgeta Hategen[†], Rama Mishra[†], Alex Polozov[†], Peng Yu[†], Emmanuel Onua[†], Jun Zhang[†], David Zembower[†], Alex Kiselyov[†], José L. Ramírez[‡], Gudmundur Sigthorsson[‡], Jon Mar Bjornsson[‡], Margret Thorsteinsdottir[‡], Thorkell Andrésson[‡], Maria Bjarnadottir[‡], Olafur Magnusson[‡], Jean-Etienne Fabre[§], Kari Stefansson[‡], and Mark E. Gurney[†,‡,*]

[†]deCODE Chemistry, 2501 Davey Road, Woodridge, Illinois 60517, [‡]deCODE Genetics, Sturlugata 8, IS-101 Reykjavik, Iceland, and [§]Institut de Génétique et de Biologie Moléculaire et Cellulaire, Institut National de la Santé et de la Recherche Médicale U596, Centre National de la Recherche Scientifique UMR7104, Université Louis Pasteur, 67400 Illkirch, France

ABSTRACT Myocardial infarction and stroke are caused by blood clots forming over a ruptured or denuded atherosclerotic plaque (atherothrombosis). Production of prostaglandin E_2 (PGE_2) by an inflamed plaque exacerbates atherothrombosis and may limit the effectiveness of current therapeutics. Platelets express multiple G-protein coupled receptors, including receptors for ADP and PGE_2. ADP can mobilize Ca^{2+} and through the P_2Y_{12} receptor can inhibit cAMP production, causing platelet activation and aggregation. Clopidogrel (Plavix), a selective P_2Y_{12} antagonist, prevents platelets from clotting but thereby increases the risk of severe or fatal bleeding. The platelet EP_3 receptor for PGE_2, like the P_2Y_{12} receptor, also inhibits cAMP synthesis. However, unlike ADP, facilitation of platelet aggregation *via* the PGE_2/EP_3 pathway is dependent on co-agonists that can mobilize Ca^{2+}. We used a ligand-based design strategy to develop peri-substituted bicylic acylsulfonamides as potent and selective EP_3 antagonists. We show that DG-041, a selective EP_3 antagonist, inhibits PGE_2 facilitation of platelet aggregation *in vitro* and *ex vivo*. PGE_2 can resensitize platelets to agonist even when the P_2Y_{12} receptor has been blocked by clopidogrel, and this can be inhibited by DG-041. Unlike clopidogrel, DG-041 does not affect bleeding time in rats, nor is bleeding time further increased when DG-041 is co-administered with clopidogrel. This indicates that EP_3 antagonists potentially have a superior safety profile compared to P_2Y_{12} antagonists and represent a novel class of antiplatelet agents.

Myocardial infarction (MI) and stroke result from acute thrombosis over ruptured or denuded atherosclerotic plaques (atherothrombosis). Atherosclerotic plaques form in the arterial vessel wall through deposition of lipids and consequent inflammatory cell infiltration (*1*). Treatment of acute thrombosis is designed either to reopen occluded arteries through mechanical revascularization and/or fibrinolysis or to prevent further atherothrombotic events by blunting platelet responses to vascular wall injury. Although the potent antiplatelet drug acetylsalicylic acid (ASA) was synthesized in the 1850s, first in France and then in Germany, and had entered widespread use as an antipyretic and analgesic by the early 1900s, recognition of its benefit for reducing risk of heart attack was slow to emerge. It was not until 1988 that the Physicians Health Study established the benefit of ASA for the prevention of heart attack (*2, 3*). This established the clinical concept that antagonism of platelet function could decrease risk of atherothrombosis while prompting the search for even more potent antiplatelet agents. Clopidogrel, an antagonist of the platelet purinergic P_2Y_{12} receptor for adenosine diphosphate (ADP), provides additional benefit over ASA for the prevention of recurrent heart attack (*4*). A more potent, second generation P_2Y_{12} antagonist, prasugrel, recently was shown to lower risk for myocardial infarction still further when compared to ASA or clopidogrel (*5*).

Unfortunately, P_2Y_{12} antagonists and ASA greatly impair normal platelet function, as shown by an increase in the risk of severe or fatal bleeding. Patients treated with prasugrel have fewer cardiac events than those tak-

*Corresponding author: mgurney@decode.com.

Received for review August 25, 2008 and accepted January 9, 2009.

Published online February 5, 2009

10.1021/cb8002094 CCC: $40.75

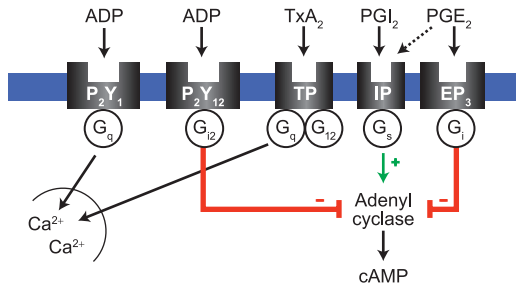

Figure 1. Adenosine diphosphate (ADP), thromboxane A_2 (TxA_2), and prostaglandin E_2 (PGE_2) act in concert to mobilize platelet Ca^{2+} and decrease adenyl cyclase activity, thereby lowering platelet cAMP and consequently triggering platelet aggregation. ADP is able to cause platelet aggregation as a sole agonist as it acts through the P_2Y_1 receptor to mobilize Ca^{2+} and through the P_2Y_{12} receptor (the target of clopidogrel) to decrease cAMP. PGE_2, which is a negative regulator of adenylyl cyclase through the EP_3 receptor, is not able to cause platelet aggregation in the absence of a co-agonist that also mobilizes Ca^{2+}. Prostacyclin (PGI_2) acting through the IP receptor, elevates cAMP and thereby is able to block the platelet agonist effects of ADP, TxA_2, and PGE_2.

ing clopidogrel, but additional patients suffer severe bleeding (*5*). For every additional cardiovascular death prevented by prasugrel, there is approximately one additional death from fatal bleeding (*5, 6*). Thus, antiplatelet therapy to reduce risk of MI and stroke could be improved if there was a means to prevent acute thrombosis over the damaged atherosclerotic plaque without prolonging bleeding.

Atherosclerotic plaque rupture or denudation of the endothelium exposes subendothelial collagen and releases von Willebrand factor, thereby providing a substrate to which platelets can adhere. Engagement of platelet glycoprotein receptors by collagen and von Willebrand factor triggers Ca^{2+} mobilization and activation of protein kinase C. Ca^{2+} mobilization in turn stimulates platelet production of thromboxane A_2 (TxA_2) and platelet degranulation to release ADP. Platelets aggregate if Ca^{2+} mobilization is accompanied by a decrease in cAMP. Platelets express multiple G-protein coupled receptors that regulate Ca^{2+} mobilization and cAMP synthesis (Figure 1). The TP receptor for thromboxane A_2 (TxA_2) and the P_2Y_1 receptor for ADP act through the G_q pathway to release intracellular Ca^{2+} stores. When Ca^{2+} mobilization is accompanied by inhibition of cAMP synthesis, platelet aggregation is induced, for example, by ADP acting through the P_2Y_{12} receptor and the inhibitory G_i protein to inhibit adenyl cyclase.

Prostanoids are formed from arachidonic acid through the concerted action of a cyclooxygenase (COX-1 or COX-2) and an appropriate synthase (*7*). When activated, platelets generate TxA_2 through COX-1 functionally coupled to thromboxane synthase. ASA prevents TxA_2 synthesis by covalently modifying COX-1 though acetylation of a serine residue in the active site. While platelets are the source of TxA_2, the healthy arterial wall is a source of prostacyclin (PGI_2). PGI_2 is produced by COX-2 functionally coupled to prostacyclin synthase. PGI_2 prevents platelet activation and aggregation in response to most agonists by acting through the IP receptor and the stimulatory G_s protein to increase adenyl cyclase activity and elevate platelet cAMP (Figure 1). The synthesis of PGI_2 by the arterial wall is inhibited by selective COX-2 inhibitors (*8*). Indeed, the importance of PGI_2 for platelet homeostasis is underscored by the increased cardiovascular risk associated with Vioxx (rofecoxib) that led to the voluntary market withdrawal of the drug in 2006.

In contrast to the healthy arterial wall, the chronic inflammatory condition of the atherosclerotic plaque leads to increased content of COX-2 and microsomal PGE_2 synthase, mPGES-1 (*9, 10*), with consequent increased production of PGE_2 (*11, 12*). PGE_2 acts at low concentrations to facilitate platelet responses to multiple agonists such as collagen, TxA_2, and ADP but has no effect on platelet aggregation in the absence of a co-agonist as it does not mobilize platelet Ca^{2+} (*13*). Four PGE_2 receptors, EP_{1-4} (*14–16*), have been identified and of these, EP_1, EP_3, and EP_4 have been shown to be present in platelets (*17*). Studies of gene-deleted mice have shown that only EP_3 mediates PGE_2 facilitation of platelet co-agonist responses (*13*). This is because, like P_2Y_{12}, EP_3 couples to the inhibitory G_i protein to inhibit adenyl cyclase and thereby decreases platelet cAMP (*13, 18*).

Gross *et al.* (*11*) recently showed that EP_3 plays a key role in atherothrombosis. In three different models of inflammatory-mediated arterial thrombosis, arachidonic acid superfusion, $FeCl_3$-mediated endothelial damage, and mechanical rupture of atherosclerotic plaque, PGE_2-promoted thrombosis was impaired if platelets lacked EP_3. Since the healthy arterial wall produces negligible PGE_2 (*11, 12*), the platelet EP_3 system should minimally affect bleeding time, although contra-

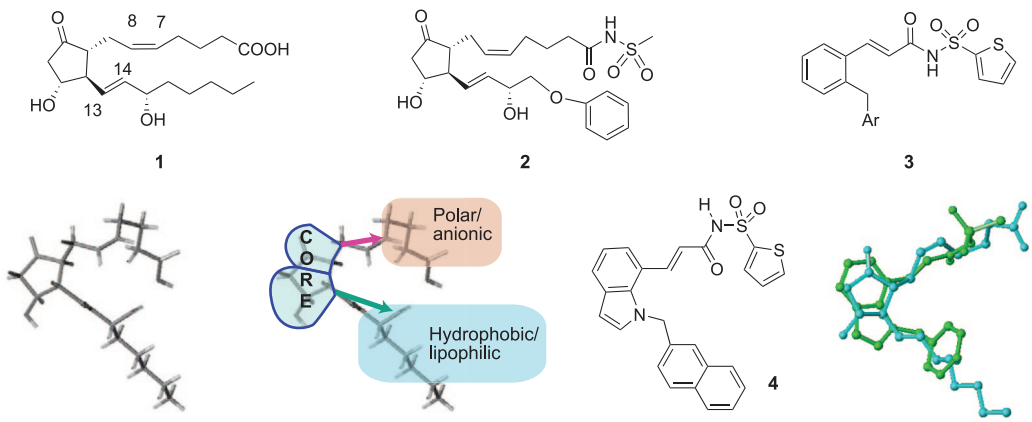

Figure 2. Use of ligand conformation to aid design of small molecule EP_3 antagonists. Top row: (1) structure of the endogenous ligand, prostaglandin E_2 (PGE_2) (*14*); (2) a potent and selective EP_3 agonist, sulprostone; (3) cinnamic acid based EP_3 antagonists reported by Juteau *et al.* (*13*). Bottom row: energy minimized conformation of PGE_2; schematic representation of the pharmacophore hypothesis and its overlay on PGE_2; compound 4, the initial hEP_3 antagonist hit with IC_{50} = 4.5 nM; overlay of the geometry optimized structures of PGE_2 (cyan) and compound 4a, (2*E*)-3-(1-benzyl-1*H*-indol-7-yl)-*N*-(thiophen-2-ylsulfonyl)prop-2-enamide) (green), based on the charge similarity index (*30, 31*).

dictory results have been reported for bleeding times in EP_3 gene-deleted mice (*13, 18*).

We now report the identification of a novel and potent EP_3 antagonist that has antiplatelet activity with minimal impact on bleeding time. These data point to EP_3 as a novel antiplatelet target in cardiovascular disease in the context of inflammatory production of PGE_2, with reduced risk of bleeding.

RESULTS AND DISCUSSION

Ligand-Based Design of EP_3 Antagonists. Our initial medicinal chemistry effort was focused on the synthesis of 1,3-disubstituted five-membered heterocycles. We reasoned that these derivatives combined features of the endogenous ligand, PGE_2, a potent and selective EP_3 agonist, sulprostone (*15*), and the cinnamic acid based EP_3 antagonists reported by Juteau *et al.* (*19*) (Figure 2). After limited structure−activity relationship (SAR) studies, however, we failed to discover compounds with potency better than 1−10 μM.

We subsequently developed a ligand-based design strategy in which we attempted to recapitulate PGE_2 pharmacophores. Specifically, we explored chemotypes featuring binding elements (*15*) that overlapped with the C7/C13 or C8/C14 atoms of PGE_2 (Figure 2). The approach yielded multiple compounds with low nanomolar potency in EP_3 binding assays as exemplified by 1,7-substituted indole **4**. In developing our structure−activity relationship (SAR) strategy, we simultaneously addressed potential metabolic liabilities of the unsubstituted indole core and developed feasible synthetic protocols. The key aspects of this are presented in Figure 3 (Areas I−IV).

To investigate structural requirements for Area I, we prepared a set of diverse bicyclic systems. Derivatives of these showed good to excellent selectivity when profiled in a panel of other EP receptors and the IP receptor. We particularly wanted at least 1000 times less potency for binding to IP versus EP_3 based on the increased cardiovascular risk found with rofecoxib (*8*). In prioritizing our chemistry efforts, we focused on 1,7-substituted indoles because of their (i) synthetic feasibility and (ii) metabolic stability upon proper substitution (Supplementary Table ST1) (*20*). We selected for further studies molecule **7** where both C3 and C5 metabolic sites of the indole were blocked with CH_3 and F, respectively. Compound **7** retained activity against EP_3 and displayed adequate stability in the rat liver microsomes assay. Of the N-substituents for Area II (Figure 3), the 2,4-dichlorobenzyl group was identified as the optimal substituent featuring >100−1000 selectivity for EP_3 versus prostanoid receptor panels. In studying binding elements within Area III, we prioritized acylsulfonamide derivatives over the parent cinnamic acid due to the ex-

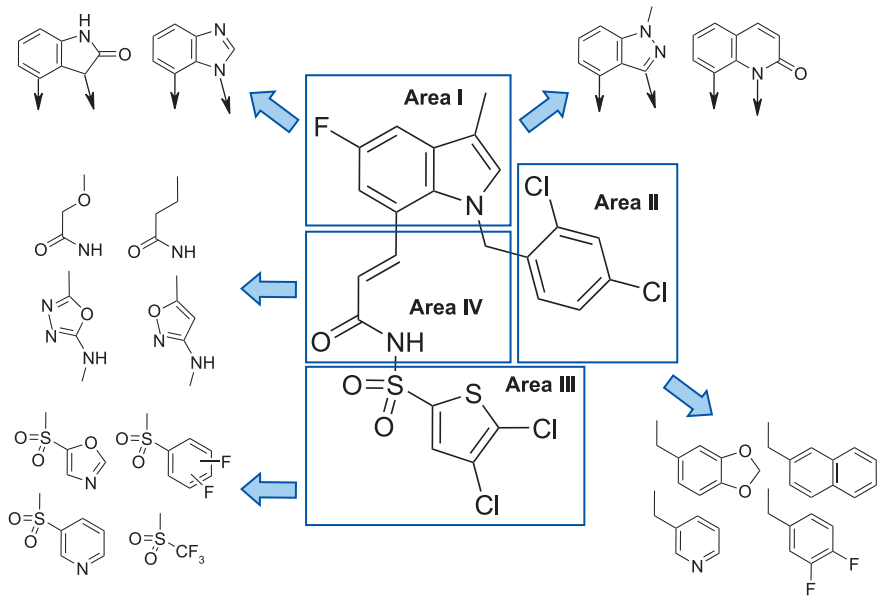

Figure 3. Strategic representation of the structure—activity relationship for different areas of the lead 1,7-indole template as discussed in the text.

tensive plasma protein binding of the latter (*19*). Furthermore, a 4,5-dichloro-2-thiophene sulfonamide group consistently featured high EP_3 potency and low fold shift (<10X) in binding assays performed in the presence of plasma proteins. Consequently, this functionality was selected as a key substituent for inclusion in subsequent compounds.

For comparison, we evaluated a cinnamic acylsulfonamide EP_3 receptor antagonist (compound **6d**) reported by Juteau *et al*. (*19*) by *in vitro* binding assay using membrane preparations derived from CHO cells stably expressing hEP_{3D} or mEP_{3a}. Compound **6d** displayed IC_{50} of 18 nM and 563 nM for human and mouse EP_3 receptors, respectively. In addition, the hEP_3 IC_{50} in the presence of 10% and 20% mouse serum was 1.19 μM (66-fold IC_{50} shift) and 4.72 μM (260-fold IC_{50} shift), respectively. Therefore, because of 30-fold lower affinity for mouse receptor and the high fold shift in the presence of plasma proteins, compound **6d** was not evaluated further.

A number of aliphatic, acyclic, and heteroaryl linkers for Area IV have been evaluated (Figure 3, Supplementary Table ST-2). In studying the optimum linker length, we found that compounds bearing a two-atom spacer (C═C, C−C, O−C, *etc.*) between the core and the acylsulfonamide group consistently displayed potent EP_3 antagonism. Compounds with longer linkers (3-atom) were less potent. Analogs with the acylsulfonamide group directly attached to the C7 of the indole did not fully displace ^{3}H-PGE_2 up to 20 μM. Disappointingly, although molecules with saturated linkers yielded good receptor affinity, their metabolic stability was consistently low (*20*). In addition, these displayed very high plasma protein binding. Insertion of aromatic linkers led to inferior potency of the resulting molecules (Figure 3). In our hands, derivatives of acrylamide (cinnamides) featured the best activity and adequate metabolic stability. We were concerned about the acrylamide double bond, as it might have the potential to covalently modify biological targets through the Michael addition reaction. We reasoned however that the chemical nature of the double bond in compound **12** (Supplementary Table ST-2) should not be a liability (*21*). Relevant synthetic papers (*22–25*) demonstrate that cinnamide is a suboptimal Michael acceptor. Also, the aryl acrylic acid anion is not likely to feature chemical or *in vivo* reactivity. Accordingly, the analog containing α,β-unsaturated acylsulfonamide provided significantly higher metabolic stability for CYP-mediated oxidative reactions, as shown in Supplementary Table ST-2.

TABLE 1. Pharmacokinetic parameters of DG-041 following intravenous and oral administration to male Sprague–Dawley rats[a]

Route	Dose (mg kg^{-1})	t_{max} (h)	C_{max} (μM)	$t_{1/2}$ (h)	$AUC_{0-\infty}$ (ng h mL^{-1})	V_{ss} (mL kg^{-1})	CL (mL h^{-1} kg^{-1})	% F
Intravenous	1.78	na	9.46 ± 0.76	2.7 ± 0.4	1447 ± 175	1790 ± 169	1250 ± 154	na
Oral	9.62	0.42 ± 0.14	2.74 ± 0.16	4.06 ± 0.99	2082 ± 453	na	na	27 ± 5.6

[a]All values are mean ± SD with $N = 3$. t_{max} = time of maximum concentration, C_{max} = maximum concentration measured, $t_{1/2}$ = terminal elimination half-life, $AUC_{0-\infty}$ = area under the curve extrapolated to infinity, V_{ss} = volume of distribution at steady-state, CL = plasma clearance.

To further confirm *in vivo* the low potential for chemical reactivity of the selected cinnamide linker, we explored the potential immunogenicity and systemic clearance of compound **12**. It was inactive in the local lymph node assay (LLNA) following topical exposure, suggesting that it did not provoke immune reactivity *in vivo*. We also labeled compound **12** with ^{14}C at the benzylic carbon for *in vivo* radiolabel distribution studies in rats testing the potential of the compound for chemical reactivity. Both male and female rats were exposed to the radioligand. At 1 h after exposure, ^{14}C radioactivity was localized to a limited number of tissues including liver, GI, and renal systems, as expected for a molecule mainly metabolized by the liver. Within 24 h radioactivity was limited to the GI tract and liver. Most of the radioactivity was excreted within 72 h with mean overall recovery of >90%. Residual radioactivity was not detected in blood, plasma, or cellular fractions. Residual radioactivity in the liver was negligibly small (0.03–0.17% between males and females), indicating the low potential of the compound for accumulation or retention through metabolic transformation into a chemically reactive species.

Pharmacokinetic data for compound **12** following intravenous and oral administration in rats are shown in Table 1 and Supplementary Figure SF-6. The apparent half-life of elimination was ~2.7 h (iv) with a systemic clearance (CL) of ~1250 mL h kg^{-1}. Clearance is greater than the estimated hepatic plasma flow rate in rats, and the volume of distribution (V_{ss}) was ~1790 mL kg^{-1}, which is larger than the estimated volume of total body water. Compound **12** is absorbed rapidly following oral administration with t_{max} at ~0.42 h and absolute oral bioavailability (%F) of ~27%.

Therefore, detailed SAR studies identified compound **12** as the lead compound for further evaluation.

***In Vitro* EP$_3$ Pharmacology.** Compound **12** (henceforth designated DG-041) displayed >1000 times selectivity in radioligand displacement binding assays against other PGE_2 receptors and against the IP receptor (Supplementary Figure SF-1A). When profiled against CHO-K1 cells expressing human or mouse EP_3, DG-041 blocked inhibition by PGE_2 of forskolin-stimulated production of cAMP (Supplementary Figure SF-1B). DG-041 also antagonized Ca^{2+} responses in FLIPR assays (Millipore) in which EP_3 activation by PGE_2 was coupled to Ca^{2+} influx (Table 2). The IC_{50} value for DG-041 against EP_3 measured in the FLIPR assay (8.1 nM) was in good agreement with the IC_{50} measured in the binding assay (4.6 nM). The compound was a full antagonist in both assays. DG-041 also was equipotent in the FLIPR assay against either PGE_2 or sulprostone, evaluating each EP_3 agonist at their EC_{80}. Binding of DG-041 to EP_3 was non-

TABLE 2. Prostanoid receptor selectivity for DG-041

Receptor	Binding assay[a] IC_{50} (nM)	FLIPR assay[b] IC_{50} (nM)
EP_1	>20,000	486
EP_2	4169	>10000
EP_3	4.6	8.1
EP_4	8039	>10000
IP	14414	>10000
FP	nd	>10000
TP	nd	742
DP_1	nd	131
$CRTH_2$	nd	>10000

[a]The following ligands were used for displacement binding assays: ^3H-PGE_2 and ^3H-Iloprost (IP). [b]The following agonists were used for FLIPR assays: EP_{1-4}, PGE_2; IP, Iloprost; FP, $PGF_{2\alpha}$; TP, U-46619; DP and $CRTH_2$, PGD_2. nd = not determined.

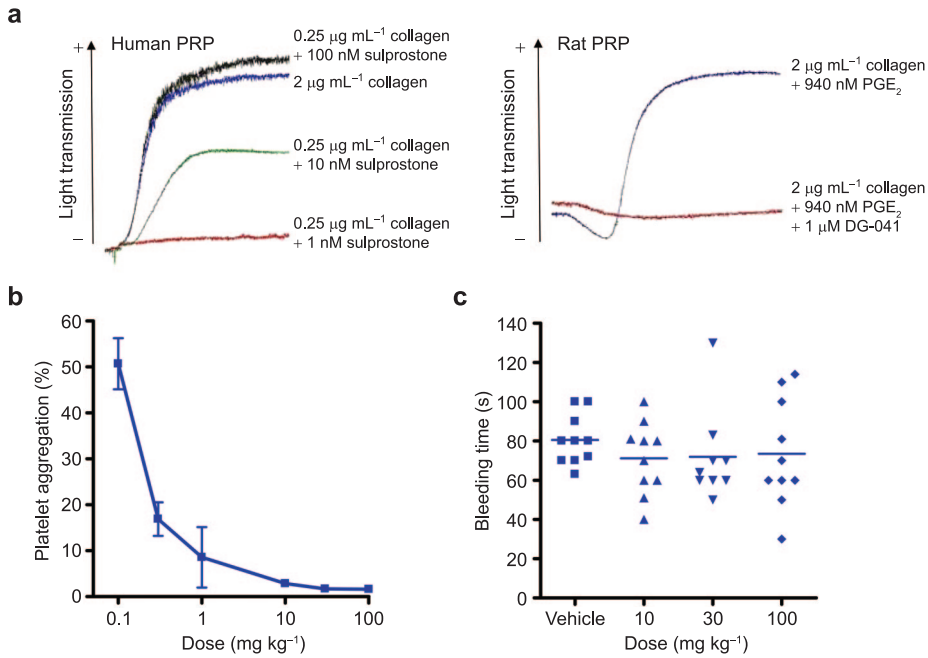

Figure 4. *In vitro* and *in vivo* pharmacology of DG-041. a) EP_3 agonists potentiate human and rat platelet aggregation in the presence of a co-agonist as measured by light transmission aggregometry of platelet-rich-plasma (PRP). Human platelets were exposed to either high or low collagen (2 or 0.25 μg mL^{-1}, respectively) in the presence of varying concentrations of sulprostone (1, 10, or 100 nM). Sulprostone dose-dependently potentiated platelet aggregation in the presence of sub-optimal collagen. Full aggregation was obtained at 100 nM sulprostone + 0.25 μg mL^{-1} collagen, similar to collagen alone at 2 μg mL^{-1}. Rat platelet aggregation similarly is facilitated by PGE_2 at sub-optimal collagen concentrations, and this is blocked by DG-041. b) DG-041 inhibits rat platelet aggregation *ex vivo*. Female Long Evans rats were gavaged with ascending doses of DG-041 in vehicle, blood samples were taken 2 h post-dose, and platelet aggregation was assessed in PRP using collagen (2 μg mL^{-1}) and PGE_2 (5 μM). Above a dose of 10 mg kg^{-1} (plasma exposure = 100 nM), rat platelet aggregation in the *ex vivo* assay was completely inhibited. The ED_{50} was 0.15 mg kg^{-1}. Data are expressed as mean ± SEM, $N = 3$. c) DG-041 does not increase bleeding time. Impact on bleeding time after surgical tail incision was assessed at doses of 10, 30, and 100 mg kg^{-1} as compared to vehicle in male Sprague—Dawley rats.

competitive with PGE_2 (Supplementary Figure SF-2). DG-041 was a less potent antagonist of the DP_1, EP_1, and TP receptors with IC_{50} = 131, 486, and 742 nM, respectively (Table 2). The free or unbound fraction of DG-041 is 0.67% in human and 1.1% in rat plasma, respectively (data not shown). The relatively high plasma protein binding for DG-041 lessens the likelihood of the compound displaying pharmacology at the DP_1, EP_1, or TP receptors. DG-041 was inactive against an extended panel of more than 50 other G-protein coupled receptors (MDS Pharma Services).

The antiplatelet activity of DG-041 was measured by light transmission aggregometry using platelet-rich plasma (PRP) from human and rat (*26*). Because PGE_2 or other EP_3 agonists alone do not induce platelet aggregation, collagen was used as a co-aggregant at sub-optimal concentration, and PGE_2 or sulprostone, a selective EP_3 agonist, were used to potentiate the aggregation response (*15, 27*). Human platelets are more sensitive to collagen than rat. This is illustrated in Figure 4. Collagen at 0.25 μg mL^{-1} fails to induce human platelet aggregation, an 8-fold higher concentration fully induces platelet aggregation, and exposure to sulprostone with the sub-optimal concentration of collagen induces the full aggregation response (Figure 4, panel a). We focused on collagen as an agonist in our experiments to mimick conditions of plaque rupture, which exposes the collagen-rich subendothelial matrix of the plaque to the platelets (*1*). PGE_2 or sulprostone also facilitate aggregation responses to multiple other platelet agonists

TABLE 3. Inhibition of human and rat platelet aggregation by DG-041 measured *in vitro*

Species	Collagen (μg mL^{-1})[a]	% Plasma	EP_3 agonist	IC_{50} (nM)[b]	N[c]
Human	0.125−0.250	100	Sulprostone (0.1 μM)	218 ± 78	8
Human	0.125−0.250	100	PGE_2 (1 μM)	130 ± 33	9
Rat	2.0	20	Sulprostone (0.2 μM)	83	1
Rat	2.0	20	PGE_2 (5 μM)	298 ± 82	3

[a]Collagen served as the primary aggregant; PGE_2 and/or sulprostone were used to facilitate platelet responses to sub-optimal collagen. [b]IC_{50} mean ± SEM were calculated across independent experiments. [c]*N* indicates the number of independent experiments performed.

at sub-optimal concentration such as ADP, the thromboxane analog U-46619, thrombin receptor activating peptide, serotonin, and platelet activating factor (*27, 28*). In assays utilizing a sub-optimal concentration of collagen and either PGE_2 or sulprostone to facilitate the collagen response, DG-041 inhibited human and rat platelet aggregation as shown for rat in Figure 4, panel a. The IC_{50} for DG-041 in human and rat platelet aggregation assays with the different EP_3 agonists are reported in Table 3.

***In Vivo* EP_3 Pharmacology and Pharmacokinetics.** We next wanted to compare and contrast an EP_3 antagonist with a P_2Y_{12} antagonist with respect to their impact on platelet function and bleeding time. Our expectation was that both receptor antagonists would decrease platelet aggregation but that only the P_2Y_{12} antagonist would prolong bleeding.

We first tested DG-041 for effects on platelet aggregation *ex vivo* and on bleeding time after surgical incision. A steep dose−response curve was observed for inhibition of platelet aggregation in rats gavaged with DG-041 with an $ED_{50} = 0.2$ mg kg^{-1} (Figure 4, panel b). Platelet aggregation was completely inhibited at a dose of 10 mg kg^{-1} or higher. DG-041 measured in the PRP sample was 0.10 ± 0.007 μM at 2 h post-dosing (10 mg kg^{-1}). No increase in bleeding time after calibrated surgical incision was noted at doses up to 100 mg kg^{-1} (Figure 4, panel c). Absorption of DG-041 became nonlinear at the top dose, reaching a plasma concentration of 19 ± 2.5 μM at 2 h or 190 times the plasma concentration needed for inhibition of platelet aggregation *ex vivo*. Thus, despite very high exposure to DG-041, we did not see an increase in bleeding time consistent with the lack of an effect on bleeding times in EP_3 null mice reported by Fabre *et al.* (*13*). While the platelet is very sensitive to the facilitation of aggregation by PGE_2 and this can be blocked by an EP_3 antagonist, this underscores how little blockade of EP_3 affects bleeding.

Clopidogrel undergoes hepatic metabolism to a chemically reactive metabolite that inactivates the platelet P_2Y_{12} receptor through covalent modification. We therefore wanted to learn if PGE_2 would restore platelet responsiveness to collagen and ADP even when the P_2Y_{12} receptor was chemically blocked. Range finding experiments with clopidogrel dosed by gavage at 2.5, 5, 10, 20, and 30 mg kg^{-1} showed that at 10 mg kg^{-1} and above clopidogrel completely blocked the *ex vivo* platelet response to varying collagen concentration (Figure 5, panel a and Supplementary Figure SF-3). At 10 mg kg^{-1}, clopidogrel also prevented platelet aggregation induced by ADP at 0.5−1 μM, but at higher ADP concentrations, efficacy was reduced (Figure 5, panel b and Supplementary Figure SF-3). Our data are similar to the clopidogrel dose−responses for collagen and ADP previously reported by Sugidachi *et al.* (*29*). Even at the minimum effective dose to prevent platelet aggregation *ex vivo*, clopidogrel significantly increased bleeding time from 80 ± 4 s in rats gavaged with vehicle to 123 ± 14 s in rats gavaged with clopidogrel ($P = 0.0149$; Figure 5, panel c). Despite the substantial blockade of P_2Y_{12} by clopidogrel at 10 mg kg^{-1}, PGE_2 restores the platelet aggregation response to both collagen and ADP (Figure 5, panels a and b). PGE_2 facilitation of the platelet response to collagen and ADP can be reversed by increasing the dose of clopidogrel to 30 mg kg^{-1}, but this further prolongs bleeding time to 4 times greater than controls (237 ± 67 s, $P = 0.0003$) (Figure 5, panel c). In the context of the inflamed plaque, production of PGE_2 may similarly limit the efficacy of antiplatelet therapy with P_2Y_{12} antagonists. Higher doses of clopi-

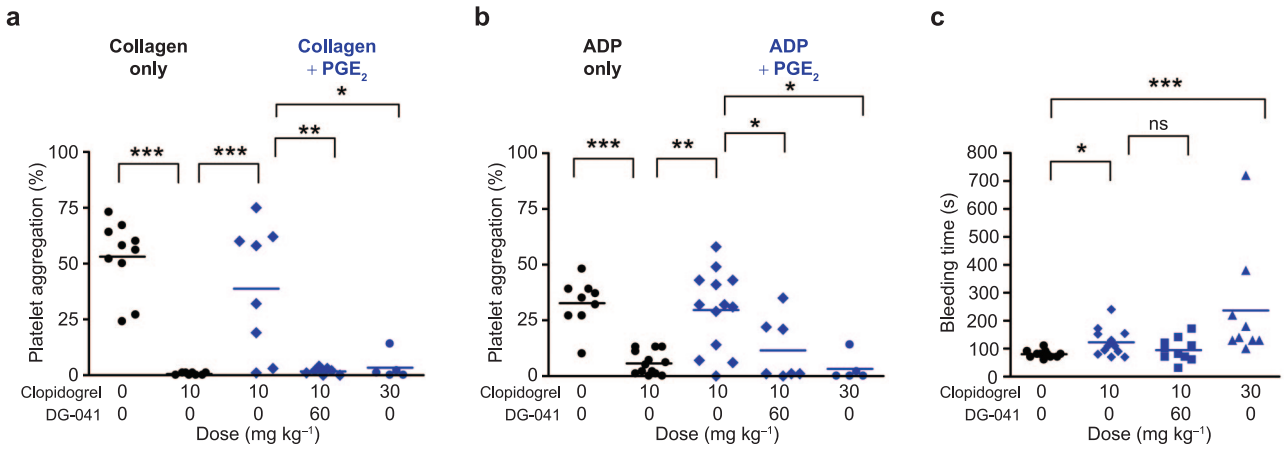

Figure 5. Effects of clopidogrel with and without co-administration of DG-041 on rat *ex vivo* platelet aggregation and on bleeding times. PRP was harvested 4 h (clopidogrel) and 2 h (DG-041) after oral administration. a) Rat platelet aggregation tested with collagen (5 μg mL^{-1}) ± PGE_2 (1 μM). Clopidogrel fully inhibited collagen-induced platelet aggregation, whereas the addition of PGE_2 restored the aggregatory effect of collagen. Co-administration of DG-041 completely blocked PGE_2-facilitated aggregation (96% reduction compared to clopidogrel alone). A similar reduction in platelet aggregation toward collagen and PGE_2 was achieved with a high dose of clopidogrel (30 mg kg^{-1}). b) Rat platelet aggregation tested with ADP (0.5 μM) ± PGE_2 (1 μM). Clopidogrel provided partial protection toward ADP-mediated platelet aggregation (83% reduction), while addition of PGE_2 reversed the inhibitory effect of clopidogrel. Combination of clopidogrel and DG-041 yielded a decrease in platelet aggregation compared to clopidogrel alone (61% reduction), whereas a high dose of clopidogrel (30 mg kg^{-1}) fully blocked aggregation. c) Clopidogrel at 10 mg kg^{-1} caused increased bleeding compared to control (from 80 ± 4 s to 129 ± 16 s), while addition of a high dose of DG-041 (60 mg kg^{-1}) did not further increase bleeding times (95 ± 13 s). Increasing the dose of clopidogrel to 30 mg kg^{-1} causes a 4-fold increase in bleeding compared to controls (237 ± 67 s).*$P < 0.05$, **$P < 0.01$, ***$P < 0.001$.

dogrel, or a more potent P_2Y_{12} antagonist such as prasugrel, may reduce PGE_2-facilitated platelet responses over the inflamed atherosclerotic plaque, but at greater risk of severe or fatal bleeding.

We then explored if DG-041 could be co-administered with clopidogrel without further prolonging bleeding, since in the human clinical setting, initial clinical trials in cardiovascular disease would likely require co-administration of DG-041 with current antiplatelet drugs. Coadministration of DG-041 at 5 or 60 mg kg^{-1} with clopidogrel efficiently inhibited PGE_2 facilitation of platelet responses to collagen and ADP (Figure 5, panels a and b and Supplementary Figure SF-4). (Doses of DG-041 greater than 60 mg kg^{-1} do not provide increased exposure due to nonlinear absorption of the compound.) PGE_2 facilitation of platelet responses to collagen were completely blocked by adding DG-041 in comparison to clopidogrel alone ($P < 0.01$), while facilitation of the platelet response to ADP was significantly reduced ($P < 0.05$). A lower dose of DG-041 (5 mg kg^{-1}) with clopidogrel also completely suppresses PGE_2 facilitation of platelet responses to collagen *ex vivo* (Supplementary Figure SF-4). Even at the deliberately high dose of 60 mg kg^{-1}, despite potentiation of the antiplatelet effect of clopidogrel, there was no further increase in bleeding time in rats gavaged with clopidogrel and DG-041 (Figure 5, panel c). This again underscores that PGE_2 activation of EP_3 plays little role in hemostasis in response to vascular breach even in the context of effective P_2Y_{12} blockade. Taken together these results suggest that co-administration of DG-041, perhaps with a lower dose of clopidogrel that has minimal effect on bleeding, could be a useful strategy for improving antiplatelet therapy in cardiovascular disease.

We successfully employed a ligand-based design strategy to develop potent antagonists of PGE_2 binding to EP_3. Early in our chemistry program, we realized that proper spatial and electronic overlap for the synthetic molecule required peri-substituted bicyclic aromatic templates. As confirmation of our ligand-based model, a broad diversity of heterocycles were tolerated by the receptor and provided potent EP_3 antagonists. Because of both synthetic considerations and potential for metabolic transformation of the central core, we focused our

efforts on SAR studies of the 1,7-disubstituted indole core. Introduction of 3-methyl and 5-fluoro substituents in the aromatic core addressed metabolic liabilities while preserving potency of the respective molecules. Addressing this issue at the earlier stages of the SAR studies allowed us to select the optimal central core for further optimization. In prioritizing our synthetic efforts, we focused on achieving optimal selectivity while reducing plasma protein binding as these parameters were reported to be a challenge for similar programs in the industry (*19*). Indole derivatives combining a lipophilic *meta/para*-substituted benzylic group at N1 with an acylsulfonamide moiety at C7 of the ring furnished the best results across multiple *in vitro* and *ex vivo* assay panels. Additional heterocyclic cores featuring the non-vicinal, peri-substitution pattern and preferred substituents resulted in active compounds with favorable *in vitro* and *ex vivo* profiles. Proper selection of the linker yielded additional advantage with regard to the metabolic stability of the final molecule. Specifically, a vinyl acylsulfonamide was identified as the optimized C7 substituent. In a comprehensive series of experiments, we confirmed the suitability of this functionality, *e.g.*, low potential for chemical reactivity, lack of antigenicity in the local lymph node assay, and lack of accumulation in ^{14}C radiolabel distribution studies in the rat. The combined SAR and *in vitro* and *ex vivo* studies yielded compound **12** (designated DG-041) as our candidate for human clinical studies. DG-041 was well tolerated in preclinical safety pharmacology and in 1 and 3 month duration chronic toxicity studies in the rat (up to 150 mg kg^{-1}) and dog (up to 20 mg kg^{-1}) following oral dosing (unpublished data). There was no evidence of bleeding in any vascular bed during the in-life phase of the chronic toxicity studies or by histopathological examination. DG-041 was not genotoxic in AMES or *in vivo* mammalian (mouse) micronucleus assays (unpublished data).

Availability of a potent and selective EP_3 antagonist allowed us to explore the pharmacology of the EP_3 signaling pathway *in vitro* and *in vivo*. Consistent with studies of platelets harvested from EP_3 null mice (*13, 18*), DG-041 is a potent inhibitor of PGE_2-facilitated responses to multiple platelet agonists when those agonists are present at sub-optimal levels. Since PGE_2 does not elicit calcium mobilization, PGE_2 is not able to trigger platelet aggregation in the absence of a co-agonist. DG-041 potently suppresses rat platelet aggregation *ex vivo* at doses above 10 mg kg^{-1} that achieve plasma levels of $\geq$0.1 μM. Even at a dose of 100 mg kg^{-1}, which gave a 190 times higher plasma concentration, no effect on bleeding time was observed after calibrated surgical incision of the tail vein. Our results in rats are consistent with the previous report by Fabre *et al.* (*13*) showing that bleeding times are unaffected in EP_3 null mice but differ from the report by Ma *et al.* (*18*), who claim that bleeding time was increased in EP_3 null mice. Since the healthy arterial wall contains only low amounts of PGE_2 (*11*) and since platelets do not produce PGE_2, blockade of EP_3 should minimally affect hemostasis and that is in fact observed. Agonists released by platelets (such as ADP and TxA_2) that amplify the response of surrounding platelets to the local environment of the fibrin clot are of overwhelming importance for hemostasis, as shown by the impact of P_2Y_{12} antagonists and COX-1 inhibitors on bleeding.

Fabre and co-workers hypothesize that production of PGE_2 differentiates acute thrombosis in the context of atherosclerotic plaque rupture from hemostasis in response to vascular breach (Fabre *et al.*, personal communication). COX-2 and mPGES-1, the biosynthetic enzymes for producing PGE_2 are expressed in atherosclerotic plaque (*9, 10*), and an increase in PGE_2 content in plaque has been reported (*11, 12*). We modeled the pro-thrombotic environment of the inflamed plaque by using PGE_2 to facilitate platelet responses to collagen. Even at the minimum effective dose of clopidogrel (10 mg kg^{-1}) that blocks *ex vivo* platelet responses to both collagen and ADP, PGE_2 is able to restore the response of clopidogrel-inhibited platelets to those agonists. We further showed that higher doses of clopidogrel can block PGE_2-facilitated responses to collagen and ADP, but at a cost. Bleeding times are even further increased, illustrating that the efficacy of clopidogrel at controlling acute thrombosis in the context of PGE_2 is limited by increasingly severe impact on hemostasis. DG-041 efficiently blocks PGE_2 facilitation of platelet aggregation, especially with respect to facilitation of a matrix signal such as collagen present in the arterial wall, and when dosed with clopidogrel, does not further prolong bleeding.

In separate studies, we show that as reported previously for EP_3 gene deletion (*11*), pharmacological blockade of EP_3 with DG-041 reduces arterial thrombosis in multiple murine models: superfusion of arachidonic acid over the carotid artery, $FeCl_3$ damage to the carotid

endothelium, and atherothrombosis in response to mechanical plaque rupture (Fabre *et al.*, personal communication). In each of these conditions, PGE_2 is produced locally and precipitates intra-arterial thrombosis in association with platelet agonists present in the vessel wall. We further show in human phase I clinical studies parallel to the preclinical studies reported herein that DG-041 does not prolong bleeding time in human subjects at doses that block PGE_2-facilitated platelet responses *ex vivo* (Human Clinical Trial DG-041-CV-013, deCODE Genetics Inc., unpublished data). Thus, an EP_3 antagonist has the potential to improve antiplatelet therapy in myocardial infarction and stroke, where control of atherothrombosis is the therapeutic goal, while minimally impacting bleeding, which limits the benefit of current antiplatelet therapy.

METHODS

Materials. Sulprostone and PGE_2 were from Cayman Chemical. Equine collagen and ADP was from Chrono-Log. 3.2% Na-citrate blood collection tubes were from Greiner Bio-One. Hydroxylpropyl β-cyclodextrin (HPβCD) was from Roquette, France. Clopidogrel/Plavix pharmacy grade tablets (75 mg) were from Sanofi Pharma-Bristol Myers Squibb. DG-041 was synthesized by deCODE Chemistry, Woodridge IL. All other buffers, salts, and reagents were from Sigma and were used as supplied.

Human *in Vitro* Platelet Aggregation Assay. Fresh blood was collected in citrated tubes by venipuncture from healthy male and female volunteers with informed consent. The subjects had not taken any nonsteroidal anti-inflammatory drugs for at least one week prior to blood collection.

Platelet-rich plasma (PRP) isolated from citrate-collected human blood was obtained after centrifugation at 100*g* for 20 min. Platelet-poor plasma (PPP) was obtained by centrifugation of PRP at 2400*g* for 10 min at 25 °C. Platelet aggregation was initiated by equine collagen (0.125−0.25 μg mL^{-1}) and PGE_2 (1 μM) or sulprostone (0.1 μM) and measured by light absorbance in a Chrono-Log model 490 stirred cell aggregometer at 37 °C for 10 min. In samples with DG-041, the antagonist was preincubated at 25 °C for 10 min.

Animals. Experiments were performed using either female Long Evans or male Sprague−Dawley rats obtained from Taconic M&B, Denmark. After shipment the animals were allowed to acclimatize for at least 5 days before use. The animals were housed under a standard 12 h light-dark cycle with free access to water and standard laboratory chow. All animal experiments were approved by the Laboratory Animal Ethical Committee in Iceland.

Dosing and Formulations. Clopidogrel/Plavix tablets (75 mg) were ground in a morter and dissolved in deionized water. The resulting supension was sonicated at 37 °C for 20 min followed by centrifugation to remove poorly soluble excipients. DG-041 was formulated in a 40% HPβCD solution in 50 mM Na-phosphate buffer, pH 7.2 for the *ex vivo* platelet aggregation experiments. For the oral route in Table 1, DG-041 was formulated in 40% HPβCD, 0.25% polyvinylpyrrolidone, 0.9% lysine hydrochloride in 50 mM Na-phosphate buffer, pH 7.2. Dosing solutions were administered orally by gavage to non-fasting rats in a dosing volume of 5−10 mL kg^{-1}. Stainless steel feeding needles (0.9 × 38 mm) and 1 mL Omnifit syringes were used for the orogastric gavage. Clopidogrel was dosed 4 h before harvesting platelets or determination of bleeding times, whereas DG-041 was dosed either 1 or 2 h before. Intravenous dosing in Table 1 was with DG-041 formulated in a 20% HPβCD solution in 50 mM Na-phosphate buffer, pH 7.2 in a dosing volume of 1 mL kg^{-1}.

Rat *in Vitro*/*ex Vivo* Platelet Aggregation Assay. Blood samples were collected by cardiac puncture while rats were under isofluran anesthesia. Blood was drawn into 10 mL syringes (Braun) with 3.2% sodium citrate buffer from blood collection tubes. PRP was obtained by centrifugation at 150*g* for 15 min at 25 °C. PPP was obtained as described above for human samples. Both PRP and PPP were diluted 1:4 with saline before use. Platelet aggregation experiments with DG-041 *in vitro* and *ex vivo* were performed as described above for human platelets, except collagen was used at 2 μg mL^{-1} and PGE_2 and sulprostone were used at 5 and 0.2 μM, respectively. Experiments with clopidogrel and a combination of clopidogrel and DG-041 were performed with collagen (2, 3.5, and 5 μg mL^{-1}) or ADP (0.5, 1, and 5 μM) as primary agonists in the absence or presence of PGE_2 (1 μM).

Bleeding Times. Bleeding time was determined in either conscious or mildly anesthetized male Sprague−Dawley rats that were immobilized in a restrainer. Anesthesia was performed using a combination of ketamine (10 mg kg^{-1}) and xylazine (10 mg kg^{-1}) in saline, administered intraperitoneally. The tail of each immobilized rat was warmed for 1 min at 40 °C and then dried. A small transverse incision was made in the middle of the tail with a scalpel. Recording of the bleeding time started when the first drop of blood touched a circular filter paper placed below the cut. Bleeding was monitored every 10 s until cessation.

Data Analysis. Platelet aggregation and bleeding time data was analyzed using Prism 4.03 for Windows (GraphPad Software). Comparison between individual groups was performed using Student's *t* test with data following normal distribution or the non-parametric Mann−Whitney test for data displaying non-gaussian distribution. Statistical significance was determined at the 5% level.

Pharmacokinetic parameters were calculated using the software WinNonlin version 4.1 for Windows. Parameters were derived using non-compartmental analysis. Data is reported as mean and standard deviation for each parameter as calculated for individual animals, $N = 3$.

General Chemistry Methods. All reagents and anhydrous solvents were obtained from commercial sources and used without further purification unless otherwise noted. NMR spectra were recorded at either 400 or 500 MHz in the solvent indicated with TMS as an internal reference. Coupling constants (*J*) are given in Hz. Column chromatography was carried out in the solvents indicated with silica gel. HPLC purity of compounds was measured with a reversed-phase HPLC (Zorbax SB-C_{18} column, 4.6 × 150 mm, 5 μm, 254 nm) with two diverse solvent systems: in system 1, compounds were eluted using a gradient elution 95/5 to 5/95 A/B over 20 min at a flow rate of 1.0 mL min^{-1} where solvent A was aqueous 0.05% TFA and solvent B was acetonitrile (0.05% TFA); in system 2, compounds were eluted using a gradient of 95/5 to 5/95 A/C over 20 min at a flow rate of 1.0 mL min^{-1} where solvent A was aqueous 0.05% TFA and solvent C was methanol. Elemental analyses were carried out by Galbraith Laboratories, Inc. (Knoxville, TN) or Midwest Microlab, LLC (Indianapolis, IN). Mass spectra were obtained using either

APCI or electrospray ionization. Schemes and synthesis of compounds are described in Supporting Information.

Acknowledgment: The authors wish to acknowledge technical contributions of J. Lin for providing guidance and overall analytical support, D. Anderson for running mass spectral analyses, and N. Zhao for acquiring NMR spectra. We also thank G. Halldórsdóttir, A. G. Hansdóttir, I. Gylfadóttir, R. Spilliaert, G. A. Pálsdóttir, B. N. Nielsen, T. Dagbjartsdottir, B. Gudmundsdóttir, S. Hrafnsdóttir, and S. Gunnarsdóttir for performance of *in vitro* and *in vivo* pharmacological assays.

Supporting Information Available: This material is available free of charge *via* the Internet at http://pubs.acs.org.

REFERENCES

1. Ross, R. (1999) Atherosclerosis—an inflammatory disease, *N. Engl. J. Med. 340*, 115–126.
2. The Physicians' Health Study: aspirin for the primary prevention of myocardial infarction, (1988) *N. Engl. J. Med.* 318, 924–926.
3. Collaborative overview of randomised trials of antiplatelet therapy—I: prevention of death, myocardial infarction, and stroke by prolonged antiplatelet therapy in various categories of patients. Antiplatelet Trialists' Collaboration, (1994) *Br. Med. J.* 308, 81–106.
4. Bhatt, D., Hirsch, A., Ringleb, P., Hacke, W., and Topol, E. (2000) Reduction in the need for hospitalization for recurrent ischemic events and bleeding with clopidogrel instead of aspirin. CAPRIE investigators, *Am. Heart J. 140*, 67–73.
5. Wiviott, S., Braunwald, E., McCabe, C., Montalescot, G., Ruzyllo, W., Gottlieb, S., Neumann, F., Ardissino, D., De Servi, S., Murphy, S., Riesmeyer, J., Weerakkody, G., Gibson, M., and Antman, E. M. (2007) The TRITON-TIMI 38 Investigators. Prasugrel versus clopidogrel in patients with acute coronary syndromes, *N. Engl. J. Med. 357*, 2001–2015.
6. Bhatt, D. (2007) Intensifying platelet inhibition—navigating between Scylla and Charybdis, *N. Engl. J. Med. 357*, 2078–2081.
7. Funk, C. D. (2001) Prostaglandins and leukotrienes: advances in eicosanoid biology, *Science 294*, 1871–1875.
8. Grosser, T, Fries, S, and FitzGerald, G A. (2006) Biological basis for the cardiovascular consequences of COX-2 inhibition: therapeutic challenges and opportunities, *J. Clin. Invest. 116*, 4–15.
9. Cipollone, F., Cesaria, P., Barbara, P., Matteo, M., Maria, F., Domenico, De C., Annalisa, I., Sante, U., Gianfranco, B., Vittorio, S., Francesco, C., Franco, C., and Andrea, M. (2001) Overexpression of functionally coupled cyclooxygenase-2 and prostaglandin E synthase in symptomatic atherosclerotic plaques as a basis of prostaglandin E(2)-dependent plaque instability, *Circulation 104*, 921–927.
10. Belton, O., Duffy, A., Toomey, S., and Fitzgerald, D. (2003) Cyclooxygenase isoforms and platelet vessel wall interactions in the apolipoprotein E knockout mouse model of atherosclerosis, *Circulation 108*, 3017–3023.
11. Gross, S., Tilly, P., Hentsch, D., Vonesch, J., and Fabre, J. E. (2007) Vascular wall-produced prostaglandin E2 exacerbates arterial thrombosis and atherothrombosis through platelet EP3 receptors, *J. Exp. Med. 204*, 3113–3120.
12. Cipollone, F., Fazia, M., Iezzi, A., Cuccurullo, C., Cesare, D., Ucchino, S., Spigonardo, F., Marchetti, A., Buttitta, F., Paloscia, L., Mascellanti, M., Cuccurullo, F., and Mezzetti, A. (2005) Association between prostaglandin E receptor subtype EP4 overexpression and unstable phenotype in atherosclerotic plaques in human, *Arterioscler., Thromb., Vasc. Biol. 25*, 1925–19331.
13. Fabre, J., Nguyen, M., Athirakul, K., Coggins, K., McNeish, J., Austin, S., Parise, L., FitzGerald, G., Coffman, T., and Koller, B. (2001) Activation of the murine EP3 receptor for PGE2 inhibits cAMP production and promotes platelet aggregation, *J. Clin. Invest. 107*, 603–610.
14. Sugimoto, Y, and Narumiya, S. (2007) Prostaglandin E receptors, *J. Biol. Chem. 282*, 11613–11617.
15. Breyer, R. M., Bagdassarian, C. K., Myers, S. A., and Breyer, M. D. (2001) Prostanoid receptors: subtypes and signaling, *Ann. Rev. Pharmacol. Toxicol. 41*, 661–690.
16. Takeuchi, K, Ukawa, H, Furukawa, O, Kawauchi, S, Araki, H, Sugimoto, Y, Ishikawa, A, Ushikubi, F, and Narumiya, S. (1999) Prostaglandin E receptor subtypes involved in stimulation of gastroduodenal bicarbonate secretion in rats and mice, *J. Physiol. Pharmacol. 50*, 155–167.
17. Paul, B., Ashby, B., and Sheth, S. (1998) Distribution of prostaglandin IP and EP receptor subtypes and isoforms in platelets and human umbilical artery smooth muscle cells, *Br. J. Haematol. 102*, 1204–1211.
18. Ma, H., Hara, A., Xiao, C. Y., Okada, Y., Takahata, O., Nakaya, K., Sugimoto, Y., Ichikawa, A., Narumiya, S., and Ushikubi, F. (2001) Increased bleeding tendency and decreased susceptibility to thromboembolism in mice lacking the prostaglandin E receptor subtype EP(3), *Circulation 104*, 1176–1180.
19. Juteau, H., Gareau, Y., Labelle, M., Sturino, C., Sawyer, N., Tremblay, N., Lamontagne, S., Carriere, M., Denis, D., and Metters, K. (2001) Structure-activity relationship of cinnamic acylsulfonamide analogues on the human EP3 prostanoid receptor, *Bioorg. Med. Chem. 9*, 1977–1984.
20. Selected compounds were incubated with rat liver microsomes and incubates were followed using LC-MS-MS analysis for metabolic profile. For example, analog **4** (Supplementary Table ST-1) showed M+16 and M+32 metabolites, consistent with mono- and bis-oxidation derived metabolites.
21. Tranilast containing an α,β-unsaturated amide functionality has been reported to be launched in Japan and Korea for the treatment of allergic rhinitis, asthma, and atopic dermatitis by Kissei Pharmaceuticals Co., Ltd. Data source http://www.iddb3.com.
22. For a report that substituents that are particularly effective in stabilizing nucleophilic addition to α,β-unsaturated carbonyl compounds include aldehydes, ketone, esters and other carboxylic acid derivatives except amide, see:Carroll, F. (1998) *Perspectives on Structure and Mechanism in Organic Chemistry*, pp 628–629, Brooks/Cole Publishing Co., Pacific Grove, CA
23. Perlmutter P. (1992) *Conjugate Addition Reaction in Organic Synthesis*, Pergamon Press, Oxford, England.
24. Palomo, C., Oiarbide, M., Dias, F., Ortiz, A., and Linden, A. (2001) *J. Am. Chem. Soc. 123*, 5602–5603. This source reports that reaction of *N*-enoly oxazolidine-2-thione with Lewis acids yields, after hydrolytic workup, the corresponding β-metcapto carbonyl adducts. This reaction represents intramolecular addition of thiol to a tertiary amide surrogate.
25. Reaction of methyl cinnamate and *O-tert*-butyldimethyl silyl cinnamate with *N*-BOC cystamine in MeOH/NaOMe for 12 h at RT provided 68% and 64% yield of the corresponding Michael adducts, respectively, whereas under similar reactions conditions neither cinnamide nor cinnamic acid yielded any desired adduct.
26. Kawasaki, T., Ozeki, Y., Igawa, T., and Kambayashi, J. (2000) Increased platelet sensitivity to collagen in individuals resistant to low-dose aspirin, *Stroke 31*, 591–595.
27. Heptinstall, S., Iue Espinosa, D., Manolopoulos, P., Glenn, J. R., White, A. E., Johnson, A., Dovlatova, N., Fox, S. C., May, J. A., Hermann, D., Magnusson, O., Stefansson, K., Hartman, D., and Gurney, M. (2008) DG-041 inhibits the EP3 prostanoid receptor—a new target for inhibition of platelet function in atherothrombotic disease, *Platelets 19*, 605–613.
28. Wise, H., Wong, Y., and Jones, R. (2002) Prostanoid signal integration and cross talk, *Neurosignals 11*, 20–28.
29. Sugidachi, A., Asai, F., Ogawa, T., Inoue, T., and Koike, H. (2000) The *in vivo* pharmacological profile of CS-747, a novel antiplatelet agent with platelet ADP receptor antagonist properties, *Br. J. Pharmacol. 129*, 1439–1446.

30. Burt, C., Richards, W. G., and Huxley, P. (1990) The application of molecular similarity calculations, *J. Comput. Chem. 11*, 1139–1146.
31. Carbo, R., Ledya, L., and Arnau, M. (1980) How similar is a molecule to another? An electron density measure of similarity between two molecular structures, *Int. J. Quantum Chem. 17*, 1185–1189.